

1 **Analysis of the thermal stability of a mercuric reductase from the Red Sea Atlantis II hot**
2 **brine environment by site-directed mutagenesis**

3 Mohamad Maged*¹, Ahmed El Hosseiny¹, Mona Kamal Saadeldin¹, Ramy K. Aziz², and Eman
4 Ramadan³

5
6 ¹Department of Biology and the Science and Technology Research Center, School of Sciences
7 and Engineering, The American University in Cairo, AUC Avenue, P. O. Box 74, New Cairo
8 11835, Egypt

9 ²Department of Microbiology and Immunology, Faculty of Pharmacy, Cairo University, 11562,
10 Cairo, Egypt

11 ³Faculty of Pharmacy, The British University in Egypt (BUE), El Sherouk City, Misr- Ismailia
12 Desert Road, Egypt

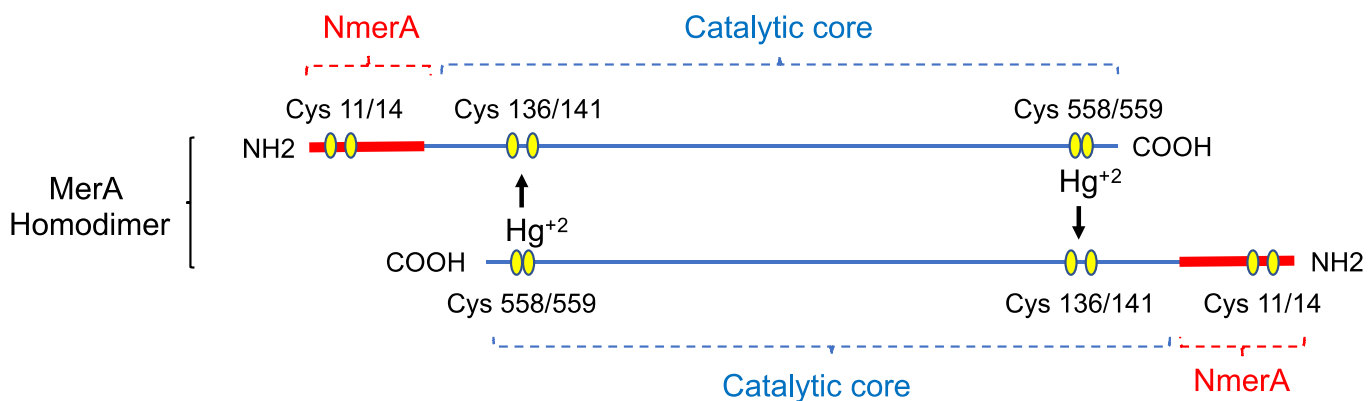
13 *To whom correspondence should be addressed:

14 Mohamad Maged

15 E-mail address: mohamadmaged@aucegypt.edu

16

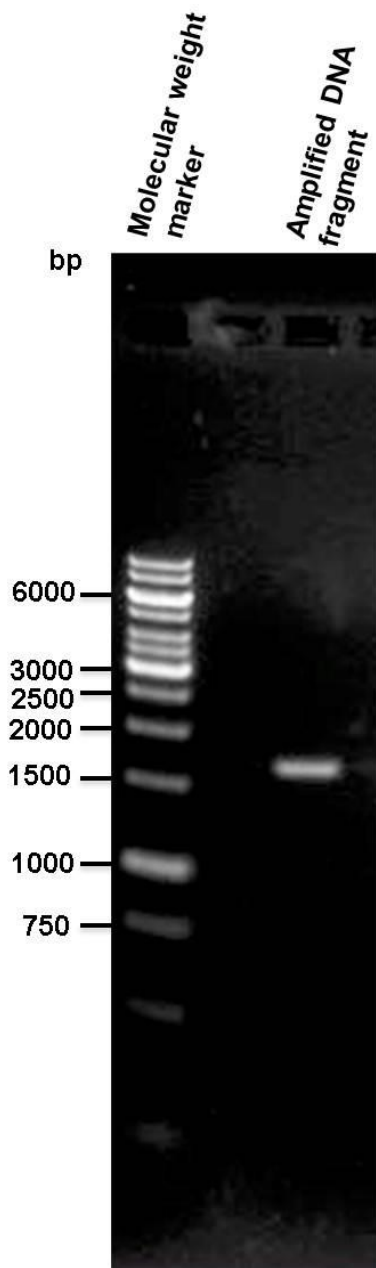
17 **Supplementary Figures**



18

19 **Fig. S1. Cartoon showing the structure of mercuric reductase dimer and the binding and**
20 **catalytic sites.**

21 This simplified diagram represents the structure of the mercuric reductase homodimer. The six
22 pairs of cysteines in the merA homodimer are highlighted in yellow, and the N-terminal domain
23 is highlighted in red. Cys 11/14 pair serves to bind Hg²⁺ and transfer it from ligands in the
24 cytoplasm to the redox-active cysteines for reduction under physiological conditions in which
25 intercellular thiols are depleted. Cys 136/141 pair is the redox-active cysteine involved in
26 catalysis. Cys 558/559 pair binds Hg²⁺ and transfers it to the active site of the other subunit for
27 reduction.



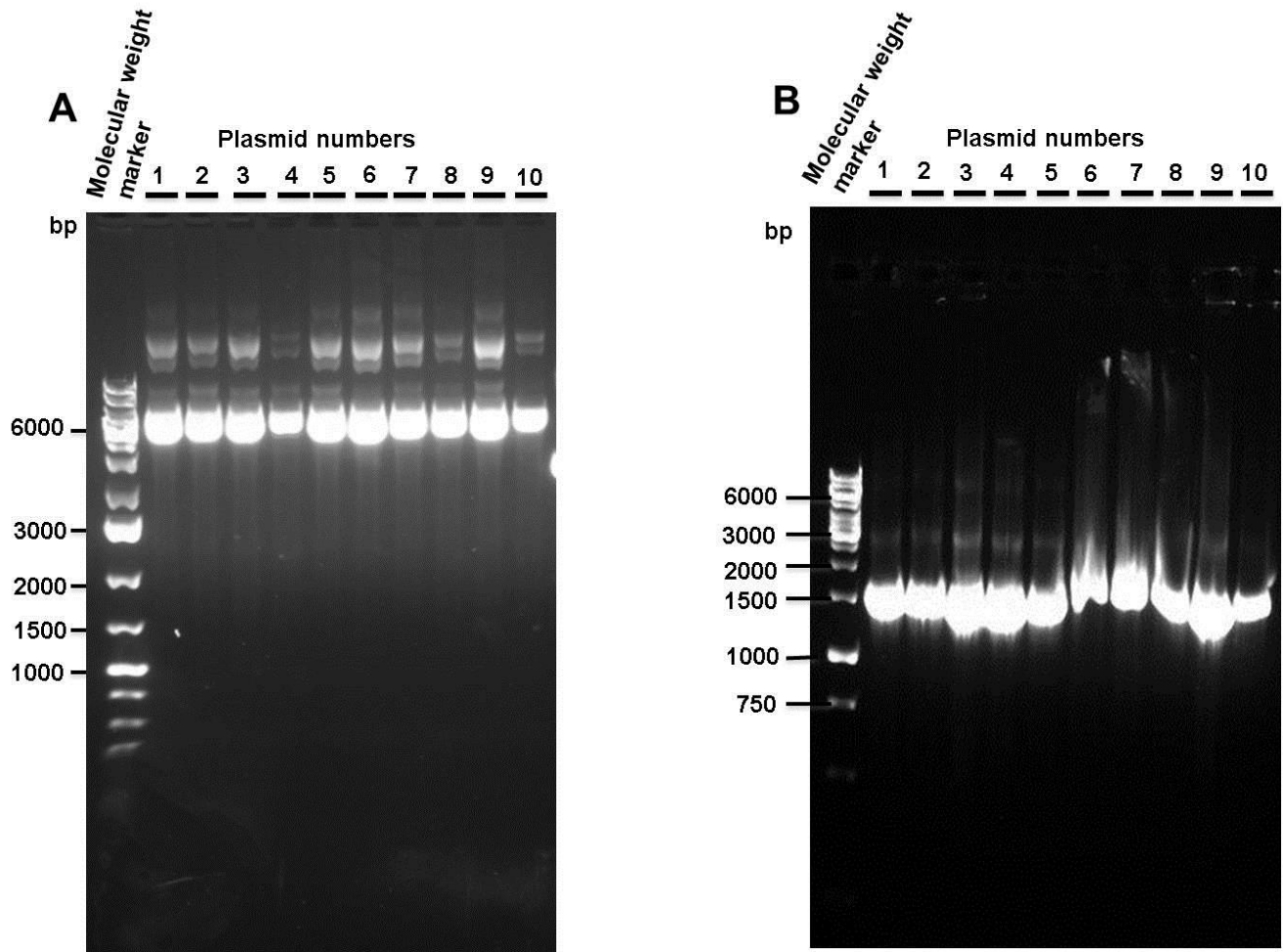
28

29 **Fig. S2. PCR amplification of metagenomic Atlantis-II LCL mercuric reductase.**

30 Products of PCR amplification of ATII-LCL metagenomic DNA analyzed on 1% agarose gel
31 electrophoresis. Lane 1, molecular weight marker; Lane 2, amplified DNA fragment.

32

33



34

35

36 **Fig. S3. Analysis of randomly selected clones from the ATII-LCL *merA* library.**

37 A) Analysis of recombinant plasmids from ten randomly selected clones on 1% agarose gel

38 electrophoresis. B) Analysis of the size of inserted DNA fragments by PCR. PCR parameter and

39 primers used in the amplification process are described in the experimental procedures section.

40 MWM refer to molecular weight marker.

41

42

1 60
 |-----|
 ATII-LCL-NH MTHLKITGHTCDSCAAHVKEALEKVPGVQSALVSYPKGTAQLAIVPGTSPDALTAAVAGL
 2A3
 2B1
 2A5
 2C6
 2A11
 2A2
 2A4

61 120
 |-----|
 ATII-LCL-NH GYKATLADAPLADNRVGLLDKVRGHWAAAEKHSGNEPPVQVAVIGSGGAAAMAALKAVEQ
 2A3
 2B1
 2A5
 2C6
 2A11
 2A2
 2A4

121 136 141 180
 |-----|
 ATII-LCL-NH GAQVTLIERGTIGGTCVNVGCVPSKIMIRAAHIAHLRRESPFDGGIARTVPTIDRSKLLA
 2A3
 2B1
 2A5
 2C6P
 2A11
 2A2
 2A4

181 240
 |-----|
 ATII-LCL-NH QQQARVDEL RHAKYEGILGGNPAITYVHGEARFKDDQSLTVRLNEGGERVVMFDRCLVAT
 2A3
 2B1
 2A5
 2C6
 2A11A
 2A2
 2A4A

241 300
 |-----|
 ATII-LCL-NH GASPAVPPIPGLKESPYHTSTEALASDTIPERLAVIGSSVVALELAQAFARLGSKVTVLA
 2A3
 2B1
 2A5
 2C6
 2A11
 2A2
 2A4A

301 360
 |-----|
 ATII-LCL-NH RNTLFFREDPAIGEAVTAAFRAEGIEVLEHTQASQVAHMDGEFVLTTHGELRADKLLVA
 2A3
 2B1
 2A5
 2C6
 2A11
 2A2
 2A4

361 420
 |-----|
 ATII-LCL-NH TGRTPNTRSLALDAAGVTYNAQGAIADIDQGHRTSNPNIIYAGDCTDQPQFYVVAARAGTR
 2A3V.....
 2B1V.....
 2A5V.....V.....
 2C6V.....
 2A11V.....
 2A2V.....T.....
 2A4V.....H.....

421 480
 |-----|
 ATII-LCL-NH AAINHTGGDAALDLTAMPVVFYVDPQVATVGYSEAEAHHDGIETDSRTLTLDNVPRALAN
 2A3
 2B1
 2A5
 2C6
 2A11
 2A2S.....
 2A4

481 540
 |-----|
 ATII-LCL-NH FDTRGFIKLVIEEGSHRLIGVQVYVPEAGELIQTAALAIRNRMTVQELADQLFPYLTHVE
 2A3
 2B1
 2A5
 2C6L.....
 2A11S.....
 2A2
 2A4A.....

541 561
 |-----|
 ATII-LCL-NH GLKLAARQTFNKDVKQLSCCAG
 2A3
 2B1A.....
 2A5
 2C6
 2A11
 2A2
 2A4

44

45

46

47

48 **Fig. S4. Multiple sequence alignment of non-redundant and full-length MerA sequences.**

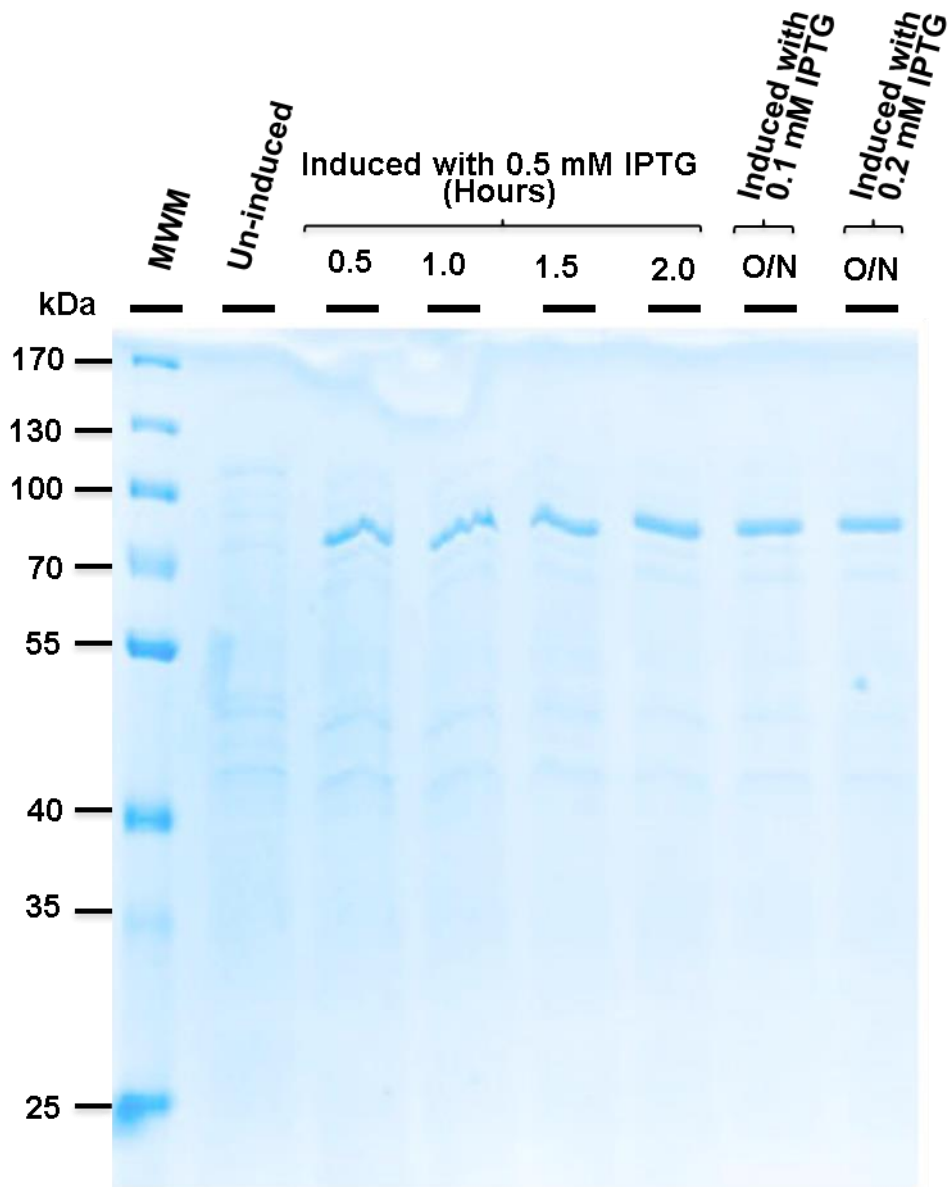
49 Multiple sequence alignment of eight non-redundant full-length MerA sequences obtained from
50 the ATII-LCL MerA library were aligned by Multalin (1). The first sequence of the figure,
51 ATII-LCL-NH, is a MerA sequence identified also in a separate library. The amino acid
52 variants/substitutions are in red letters. The NmerA domain (2) is underlined in green. The
53 Dimerization domain (3) is underlined in purple.

54

55

56

57



58

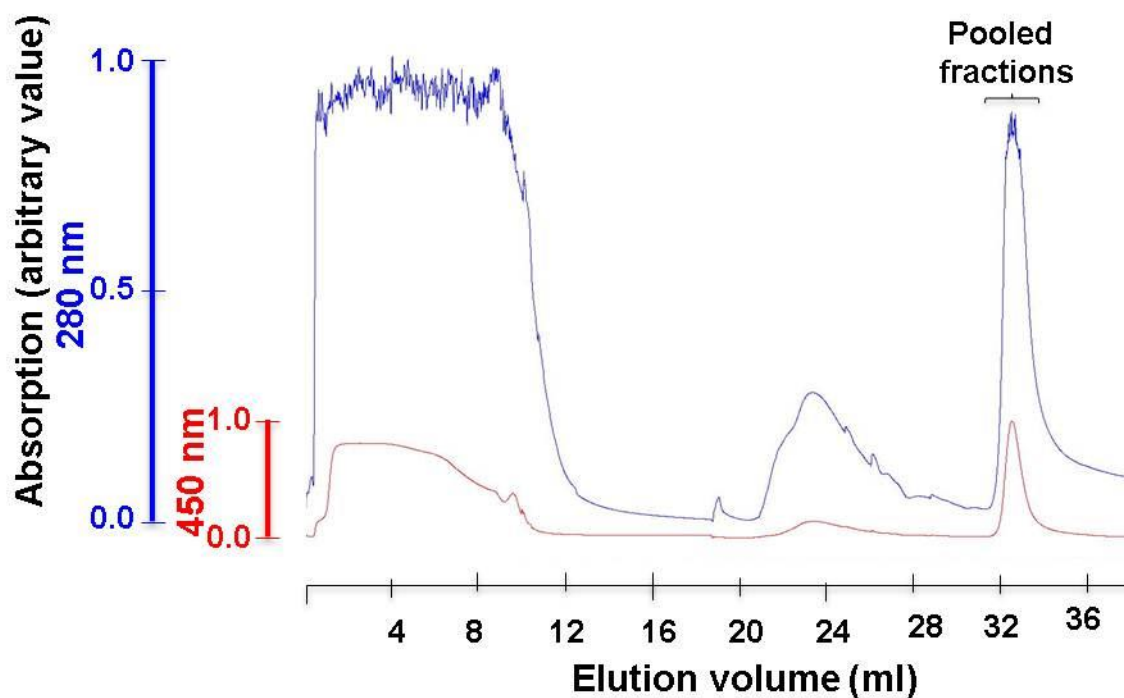
59 **Fig. S5. Induction of ATII-LCL-NH MerA at different conditions.**

60 SDS-PAGE 10% of the induced ATII-LCL-NH-merA gene was performed as described in the
 61 figure. First lane is the molecular weight marker (MWM).

62 .

63

64

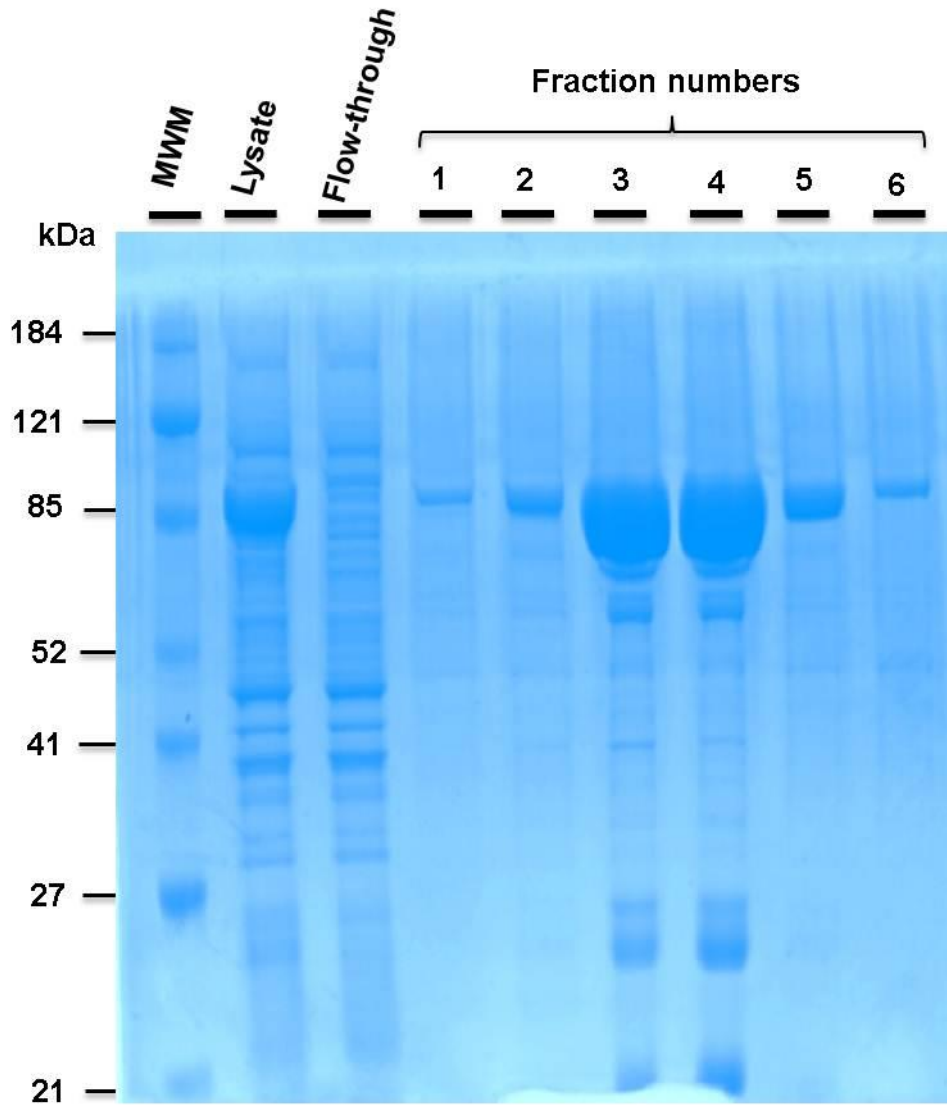


65

66 **Fig. S6. Purification profile of MerA ATII-LCL-NH recombinant enzyme using HisTrap**
67 **affinity column.**

68 The ATII-LCL-NH *E. coli* cell lysate was uploaded into 1 ml HisTrap column equilibrated with
69 40 mM imidazole using the AKTA purifier machine. On-line AKTA monitor adjusted at 280 nm
70 and 450 nm was used to follow the elution profile of proteins and FAD respectively. 250 μ l
71 aliquots were collected in each fraction. Elution of the protein was achieved by changing the
72 buffer to 500 mM imidazole at 28 ml of the elution volume. Pooled fractions containing ATII-
73 LCL-NH MerA are indicated in the figure.

74

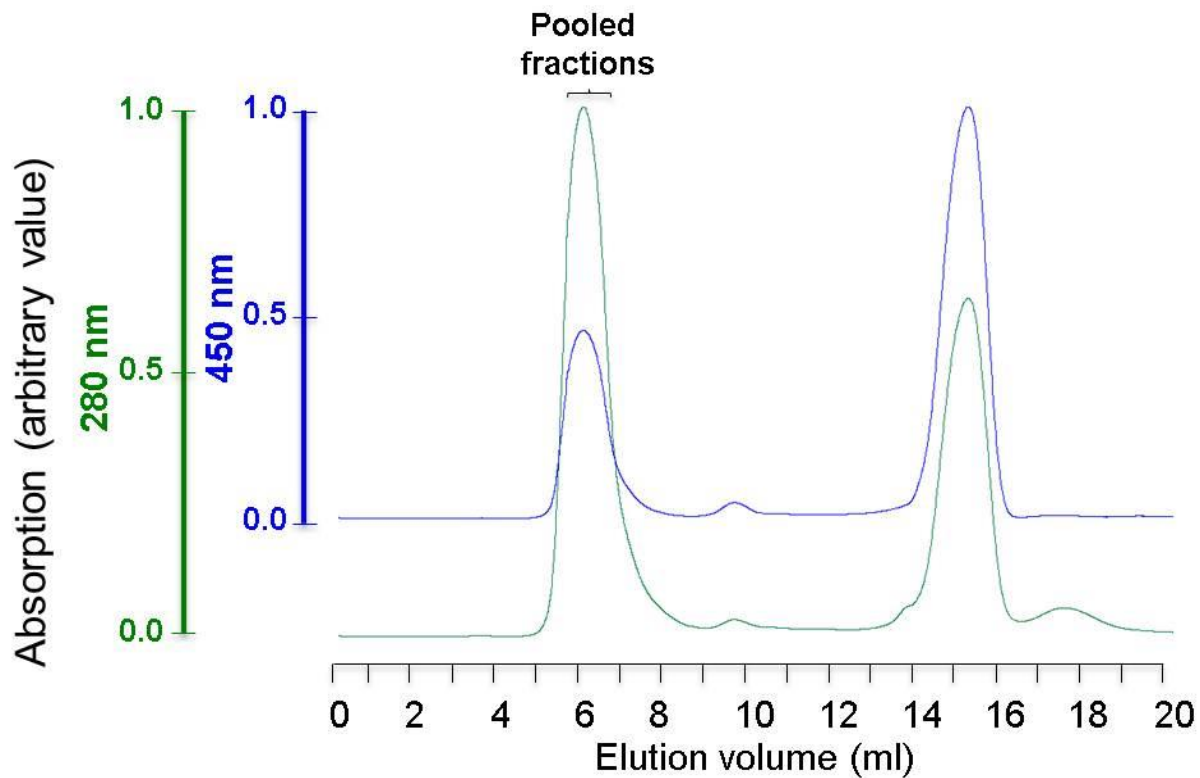


75

76 **Fig. S7. Visualization of the HisTrap purification process by SDS-PAGE.**

77 Aliquots from the HisTrap purification process were analyzed by SDS-PAGE as described in the
78 experimental procedures. Fractions 1 to 6 refer to the pooled fractions indicated in Fig. S6.

79



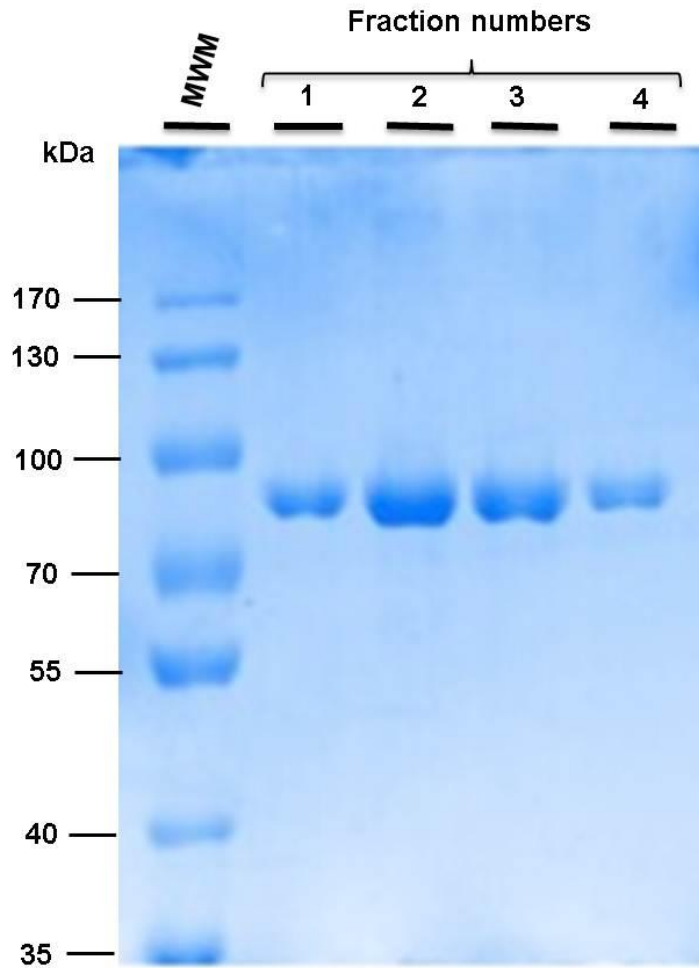
80 .

81 **Fig. S8. Purification profile of MerA ATII-LCL-NH recombinant enzyme on Superdex 75**
 82 **column.**

83 Pooled fractions from the HisTrap column were uploaded into 24-ml Superdex column
 84 equilibrated with PBS buffer using the AKTA purifier machine. On-line AKTA monitor adjusted
 85 at 280 nm and 450 nm was used to follow the profile of elution of proteins and FAD
 86 respectively. Aliquots, 250 μ l, were collected. Pooled fractions are indicated in the figure.

87

88

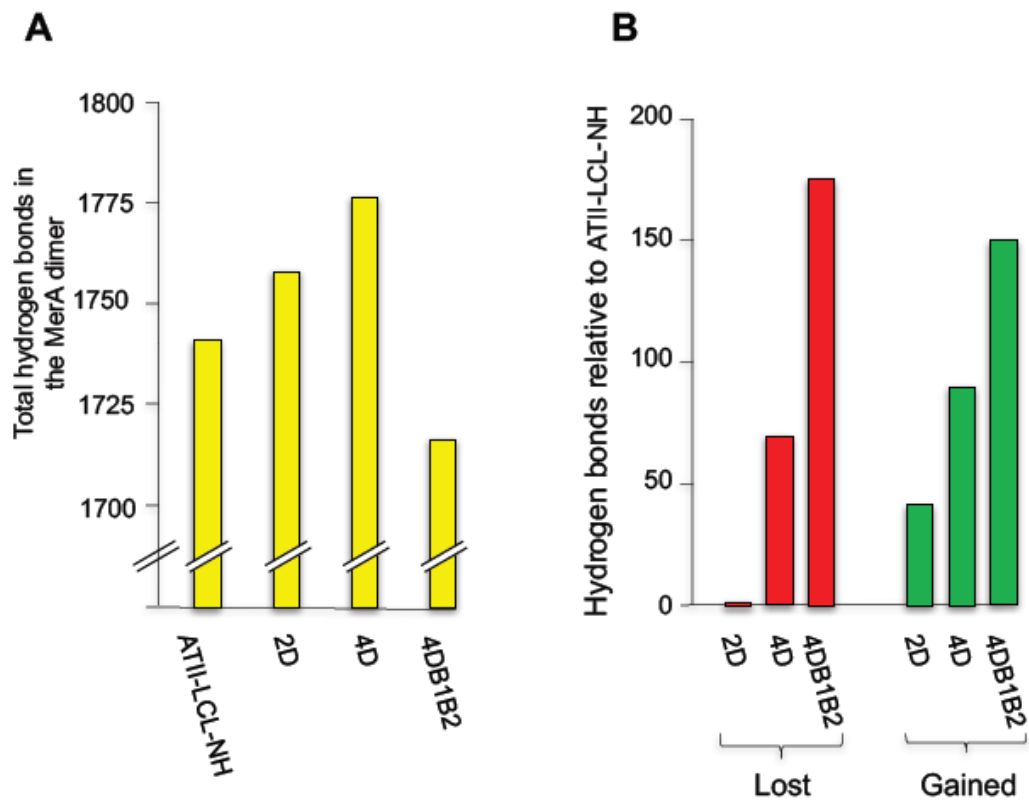


89

90 **Fig. S9. Assessment of Superdex 75 purification process by SDS-PAGE.**

91 Aliquots from the Superdex 75 purification process were analyzed on 10% SDS-PAGE as
92 indicated in the experimental procedures. Fractions 1 to 4 refer to the pooled fractions indicated
93 in Fig. S8.

94



95

96 **Fig. S10. Total hydrogen bonds of ATII-LCL-NH and its mutants.**

97 A) Total hydrogen bonds in the indicated MerAs were calculated by Hydrogen Bond Calculator

98 version 1.1 (4). B) The loss and gain of hydrogen bonds in each MerA indicated in the figure

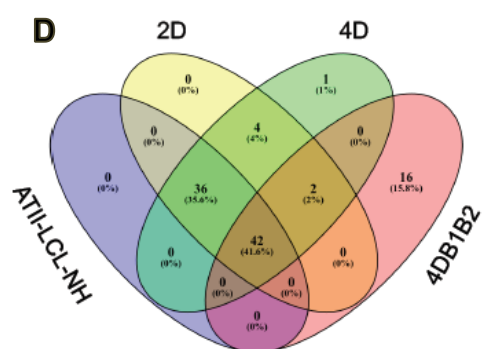
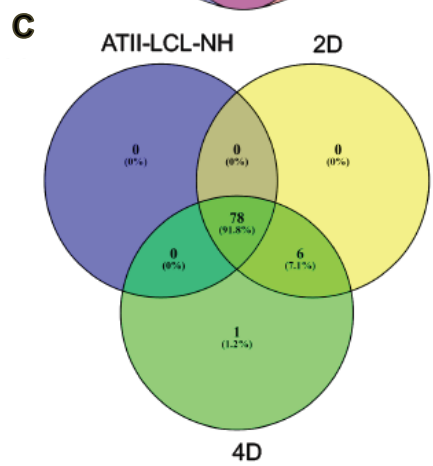
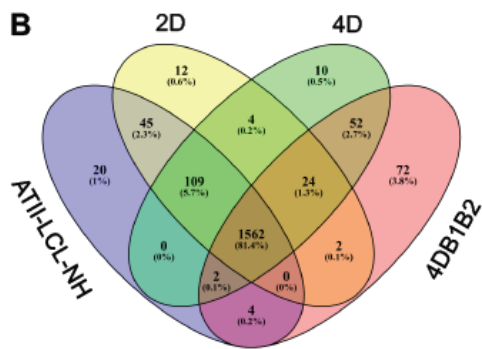
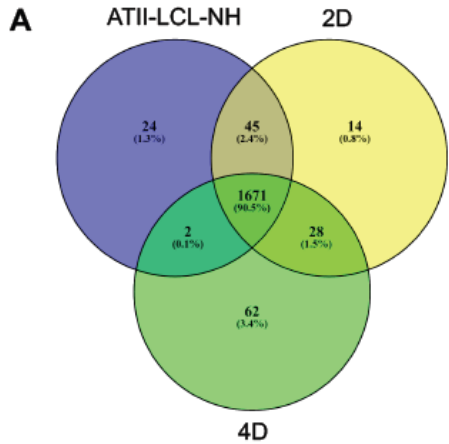
99 were computationally calculated.

100

101

102

103



104

105

106 **Fig. S11. Venn diagram of hydrogen bonding and salt bridges in ATII-LCL-NH**
107 **and its mutants.**

108 Venn diagrams of total hydrogen bonds and salt bridges in ATII-LCL-NH, 2D, and 4D mutants
109 were created and drawn using Venny software version 2.1 (5). A) Diagram of total potential
110 hydrogen bonds in ATII-LCL-NH and 2D mutant. B) Diagram of ATII-LCL-NH together with
111 2D, 4D, and 4DB1B2 mutants. C) A Venn diagram of total potential salt bridges in ATII-LCL-
112 NH and 2D mutant. D) Diagram of ATII-LCL-NH together with 2D, 4D, and 4DB1B2 mutants.

113

114

115

116

117

118

119

120

121

```

001 Input_pdb_SEORES_A      L D A A G V T V N A Q - G A I V I D Q G M R T S N P N I Y A A G D C - - - - T D Q P - Q F V Y V A A
002 UniRef90_Q51772_86_548  L D A P G V T V N A Q - G A I V I D Q G M R T S N P N I Y A A G D C - - - - T D Q P - Q F V Y V A A
003 UniRef90_A0A2S5LUM8_99_561 L D A A G I T V N L Q - G A I V I D P G M R S S V E H I Y A A G D C - - - - T D Q P - Q F V Y V A A
004 UniRef90_A0A2N1XUH0_8_470  L E A A G V A V N T Q - G A I V I D Q G M R T S T P H I Y A A G D C - - - - T D Q P - Q F V Y V A A
005 UniRef90_U2HNM8_98_560    L E A A G V V V N K Q - G A I E I D P G M R T S A P D I Y A A G D C - - - - T D Q P - Q F V Y V A A
006 UniRef90_A0A2S0MY95_14_475 L E A A G V A I D A Q - G A I A I D T G M R T S A P H I Y A A G D C - - - - T D L P - Q F V Y V A A
007 UniRef90_A0A0M1EG14_101_564 L D A A G V V V N A Q - G A I T I D H A M R T T V P H I Y A A G D C - - - - T D Q P - Q F V Y V A A

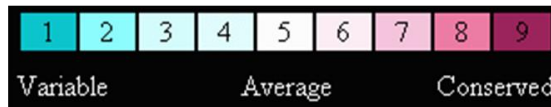
```

Four Alanines 414-417

```

001 Input_pdb_SEORES_A      A A G T R A A I N M T - - - - G G - - - D A A L D - - L T A M P A V V F T D P Q V A T V G Y S E A
002 UniRef90_Q51772_86_548  A A G T R A A I N M T - - - - G G - - - D R A L N - - L T A M P A V V F T D P Q V A T V G Y S E A
003 UniRef90_A0A2S5LUM8_99_561 A A G T R A A I N M T - - - - G G - - - D A A I D - - L T A M P A V V F T D P Q V A T V G Y S E A
004 UniRef90_A0A2N1XUH0_8_470  A A G T R A A I N M T - - - - G G - - - D A A L D - - L S A M P A V V F T D P Q V A T V G Y S E A
005 UniRef90_U2HNM8_98_560    A A G T R A A L N M T - - - - G G - - - D A A L D - - L T A V P A V V F T D P H V A T V G L S E Q
006 UniRef90_A0A2S0MY95_14_475 A A G T R A A I N M T - - - - G G - - - D A A I D - - L A A M P A V V F T D P Q V A T V G R S E A
007 UniRef90_A0A0M1EG14_101_564 A A G T R A A I N M T - - - - G G - - - N A T L D - - L T A M P A V V F T D P Q V A T V G Y S E A
008 UniRef90_A0A0J8PU16_99_562 A A G T R A A I N M T - - - - G G - - - D A A L D - - L T A M P A V V F T D P Q V A T V G Y S E A

```



122

123

124 **Fig. S12. ConSurf Alignment of ATII-LCL-NH MerA model and homologous mercuric**
 125 **reductases.**

126 ConSurf software (6) was used to calculate and analyse the evolutionary conservation of every
 127 amino acid. Ala 414 is highlighted in dark purple indicating its highest conservation among
 128 homologous mercuric reductase enzymes, while Ala 416 is highlighted in white denoting its
 129 average variability. A color-coded key is provided.

130

131

132

133

134

135

136

137

138

139 **Supplementary figures references**

140

141 1. Corpet F. 1988. Multiple sequence alignment with hierarchical clustering. *Nucleic*
142 *Acids Res* 16:10881-90.

143 2. Ledwidge R, Hong B, Dotsch V, Miller SM. 2010. NmerA of Tn501 mercuric ion
144 reductase: structural modulation of the pKa values of the metal binding cysteine
145 thiols. *Biochemistry* 49:8988-98.

146 3. Zhang Y, Bond CS, Bailey S, Cunningham ML, Fairlamb AH, Hunter WN. 1996.
147 The crystal structure of trypanothione reductase from the human pathogen
148 *Trypanosoma cruzi* at 2.3 Å resolution. *Protein Sci* 5:52-61.

149 4. Petsko GA, Ringe D. . 2004. Bonds that stabilize folded proteins, p 10-11,
150 *Protein Structure and Function*. New Science Press.

151 5. Oliveros JC. 2007-2015. Venny. An interactive tool for comparing lists with
152 Venn's diagrams. <http://bioinfogp.cnb.csic.es/tools/venny/index.html> Accessed

153 6. Celniker G, Nimrod G, Ashkenazy H, Glaser F, Martz E, Mayrose I, Pupko T,
154 Ben-Tal N. 2013. ConSurf: Using Evolutionary Data to Raise Testable
155 Hypotheses about Protein Function. *Israel Journal of Chemistry* 53:199-206.

156